# Direct three-dimensional patterning using nanoimprint lithography

Mingtao Li,[a] Lei Chen, and Stephen Y. Chou
*NanoStructure Laboratory, Department of Electrical Engineering, Princeton University, Princeton, New Jersey 08544*

(Received 27 February 2001; accepted for publication 5 April 2001)

We demonstrated that nanoimprint lithography (NIL) can create three-dimensional patterns, sub-40 nm T-gates, and air-bridge structures, in a single step imprint in polymer and metal by lift-off. A method based on electron beam lithography and reactive ion etching was developed to fabricate NIL molds with three-dimensional protrusions. The low-cost and high-throughput nanoimprint lithography for three-dimensional nanostructures has many significant applications such as monolithic microwave integrated circuits and nanoelectromechanical system. © *2001 American Institute of Physics.* [DOI: 10.1063/1.1375006]

Conventional lithography creates two-dimensional patterns in a resist film. To create three-dimensional patterns, multiple lithography with alignment or single lithography with multi-layer resists is required. For example, sub-quarter micron T-gates were fabricated by electron beam lithography[1–6] or by its combination with photolithography[7,8] in a multilayer resist system. Another example that will benefit from advantages of direct three-dimensional patterning is the air-bridged structures widely used in monolithic microwave integrated circuit (MMIC)[9,10] and nanoelectromechanical system[11–14] (NEMS). For mass manufacturing, a cost effective three-dimensional nanofabrication technique is preferable.

Nanoimprint lithography (NIL)[15] has been used as a sub-10 nm resolution[16] patterning technology with low-cost and high-throughput. Previously, NIL was used in patterning planar nanostructures in resist. In this letter, we present the demonstration of NIL in patterning three-dimensional nanostructures, in particular with sub-40 nm metal T-gates and an air-bridge structure.

The first step in our processing is to fabricate molds, using electron beam lithography and reactive ion etching (RIE). For making a T-gate mold, our approach is to make T-shaped metal structures on mold surface first, and then transfer them to upside down T-shaped mold protrusions. The details of mold fabrication are shown schematically in Fig. 1. A silicon wafer with a 420 nm thermal oxide was used as mold substrate. To create three-dimensional openings by one single step electron beam lithography, a bilayer of electron sensitive resists was employed. It consisted of a 40 nm 950 000 molecular weight polymethyl methacrylate (PMMA) bottom layer and 120 nm P(MMA-MAA) copolymer top layer. Each coating step was followed by a 30 min. bake at 165 °C and atmosphere ambient. A 35 keV electron beam was then used to define patterns according to the self-aligned exposure scheme shown in Fig. 2(a) with T-gate footprints having high dose exposure and top caps low dose exposure. Since P(MMA-MAA) has a higher exposure sensitivity, low dose exposure (0.2 nC/cm) only opens trenches in P(MMA-MAA) after development, while high dose (1.0

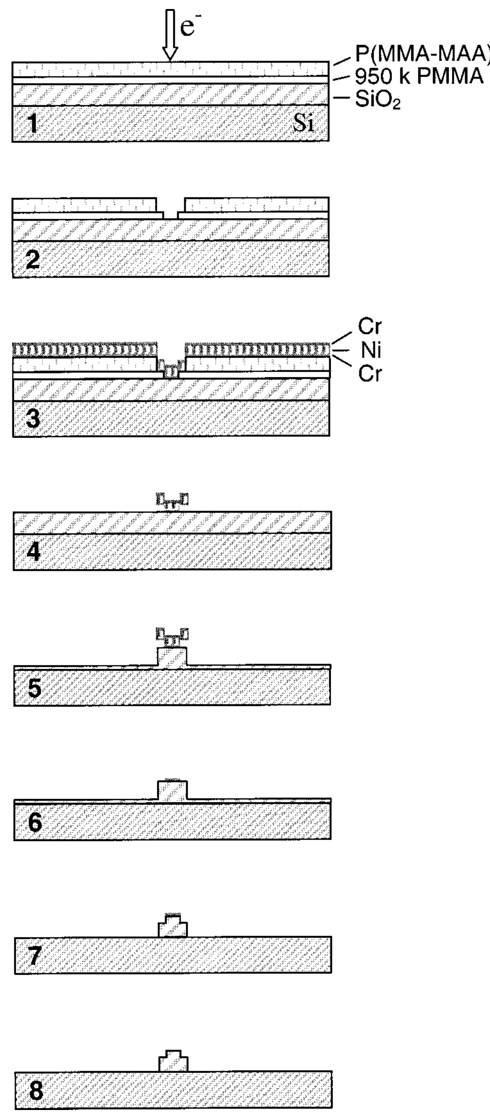


FIG. 1. Schematic of T-gate mold fabrication for nanoimprint lithography: (1) pattern definition by electron beam lithography, (2) develop to create a three-dimensional resist opening, (3) metal deposition, (4) lift-off in acetone, (5) RIE to transfer T-gate top cap to oxide, (6) Ni removal in nitric acid, (7) RIE to transfer T-gate footprint to oxide, and (8) Cr removal in CR-7.

[a]Electronic mail: mtli@ee.princeton.edu

 

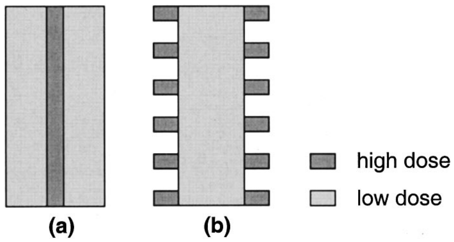


FIG. 2. Electron beam exposure schemes of (a) T-gate and (b) air-bridge. For T-gate definition, high dose is used for exposing footprints and low dose for top caps. For air-bridge, bridge posts and span receive high dose and low dose exposure, respectively.

nC/cm) opens trenches in both layers. T-shaped three-dimensional openings were created in P(MMA-MAA)/PMMA, after being developed in methanol/2-proponal (volume ratio 1:1) at room temperature. With the evaporation of 10 nm chromium (Cr), 35 nm nickel (Ni), 15 nm chromium, and lift-off in acetone, T-shaped metal masks were created. Chromium serves as an etching mask, and nickel as a sacrificial layer used to change the shape of metal mask in the following process. Reactive ion etching with $CF_4/H_2$ gas chemistry was used twice to transfer these metal T-gates to oxide. A wide rectangular oxide beam (T-gate top cap) was formed by the first etching step. The nickel layer was then dissolved in the diluted nitric acid, resulting in T-shaped metal masks being transformed to narrow Cr stripes. After the second etching step, a narrower oxide beam (T-gate footprint) was created on the wide rectangular oxide beam. An

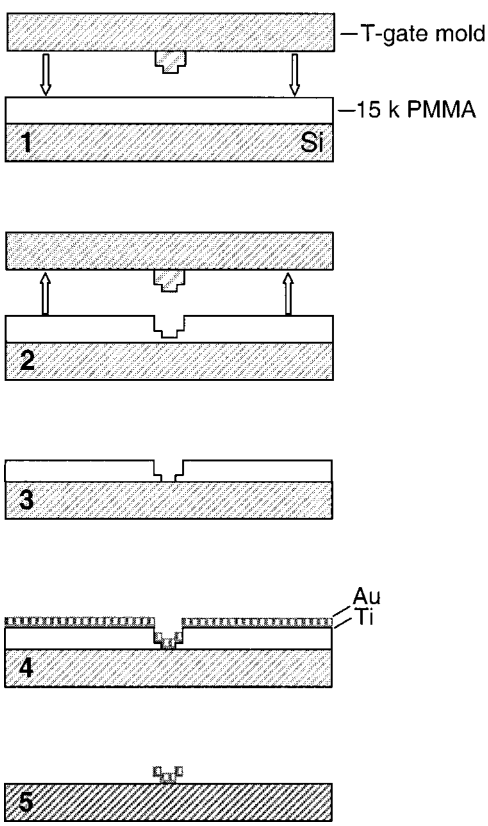


FIG. 3. A schematic of T-gate fabrication by nanoimprint lithography: (1) and (2) imprint using a T-gate mold to create a three-dimensional opening in PMMA; then separate mold from substrate, (3) pattern transfer down to PMMA through oxygen plasma to remove the residual PMMA at the trench bottom, (4) metal deposition, and (5) lift-off in acetone.

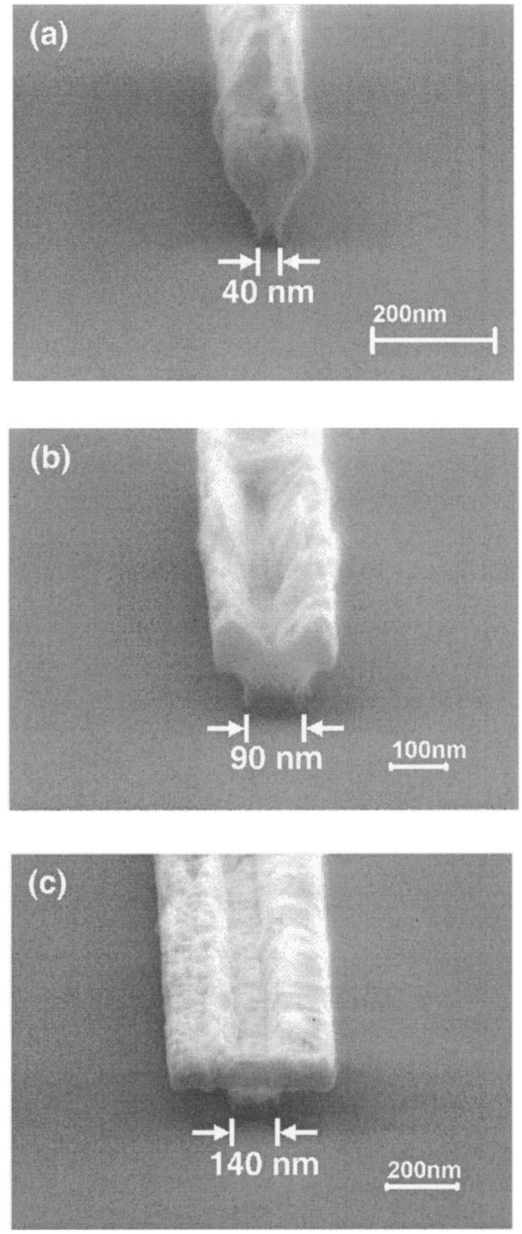


FIG. 4. Metal T-gates with a (a) 40, (b) 90, and (c) 140 nm footprint, fabricated by nanoimprint lithography and lift-off.

upside down T-shaped oxide protrusion was thus produced. Finally Cr stripes were stripped off in chromium etchant (CR-7). T-gates with different sized footprints were patterned on one mold.

To make an air-bridge mold, the same processing as above was used. Figure 2(b) shows the scheme for electron beam lithography, with bridge posts receiving high dose exposure and bridge span having low dose exposure. Air-bridged metal masks standing on an oxide surface were created after development, metal evaporation (Cr/Ni/Cr), and lift-off. Two RIE steps were then used to transfer them to upside down air-bridged oxide protrusions. The fabrication of T-gate and air-bridge mold shows that free-standing metal masks can also guarantee optimal etching anisotropy with an optimized etching recipe being used.

The molds were then used to imprint 520 nm thick 15 000 molecular weight PMMA spun on a silicon substrate. After the residual PMMA at trench bottom is removed by

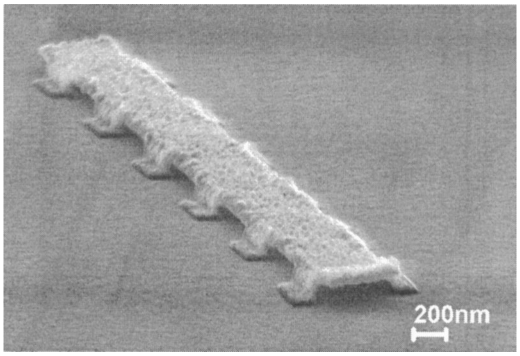


FIG. 5. Metal air-bridge structure fabricated by nanoimprint lithography and lift-off.

oxygen RIE, PMMA templates were transferred to metals by evaporation of titanium (Ti) and gold (Au), and lift-off. Titanium promotes adhesion between gold and silicon substrate. Figure 3 summarizes metal T-gate fabrication by nanoimprint lithography and lift-off. The same processing was applied to air-bridge fabrication. A parallel-plate imprint machine was used. The imprint temperature and pressure were 175 °C and 645 psi, respectively. Mold and substrate separation is easy.

Figure 4 shows metal T-gates fabricated by nanoimprint lithography and lift-off, with a 40, 90, and 140 nm footprint, respectively. With our sub-40 nm T-gate technology, metal–semiconductor field effect transistors (MESFETs) with high working frequency and low noise can be fabricated. To obtain better high frequency performances, an etching recipe resulting in tapered sidewalls can be used for footprint transfer during mold fabrication to reduce parasitic inductance due to sharp corners between T-gate footprint and substrate. Compared to conventional ways of patterning sub-quarter micron T-gates, NIL approach with proper processing is much simpler, faster, and cheaper.

An air-bridge structure fabricated by NIL is shown in Fig. 5. It was released after the deposited metals were lifted off in warm acetone. Posts are 150 by 400 nm, and the bridge stands about 110 nm above substrate. Depending on applications, scaling down to smaller dimensions is not a problem.

While all of these three-dimensional nanostructures are fabricated out of polymer templates, ceramic (such as $SiO_2$) templates can be used wherever necessary. NIL[17] is capable of directly patterning $SiO_2$ gel films prepared by sol-gel technique, so sacrificial layers which can sustain high temperature processing are available. NIL is promising in making NEMS elements, combined with surface micromachining technique.

Our molds with three-dimensional protrusions were made using conventional electron beam lithography, but they can imprint three-dimensional nanostructures much faster than conventional nanofabrication techniques. More important, these molds can be used repeatedly, thus counteracting processing efforts to fabricating them. Due to simplified processing steps of making these three-dimensional nanostructures, low-cost and high-throughput are guaranteed when using NIL. Besides these advantages crucial for future mass production, high resolution is maintained as well during imprinting, with the fabrication of sub-40 nm T-gates being an example.

In conclusion, we demonstrated the feasibility of sub-40 nm T-gates and air-bridge fabrication using nanoimprint lithography at low-cost and high-throughput. Nanoimprint lithography is one potential technology for fabricating three-dimensional nanostructures.


[1] A. S. Wakita, C.-Y. Su, H. Rohdin, H.-Y. Liu, A. Lee, J. Seeger, and V. M. Robbins, J. Vac. Sci. Technol. B **13**, 2725 (1995).

[2] R. Grundbacher, C. Youtsey, and I. Adesida, Microelectron. Eng. **30**, 317 (1996).

[3] R. Cheung, W. Patrick, I. Pfund, and G. Hähner, J. Vac. Sci. Technol. B **14**, 3679 (1996).

[4] R. Grundbacher, I. Adesida, Y.-C. Kao, and A. A. Ketterson, J. Vac. Sci. Technol. B **15**, 49 (1997).

[5] M. M. Ahmed and H. Ahmed, J. Vac. Sci. Technol. B **15**, 306 (1997).

[6] D. Via, C. Bozada, C. Cerny, G. DeSalvo, R. Dettmer, J. Ebel, J. Gillespie, T. Jenkins, K. Nakano, C. Pettiford, T. Quach, and J. Sewell, J. Vac. Sci. Technol. B **15**, 2916 (1997).

[7] Y. Anda, T. Matsuno, M. Tanabe, T. Uda, M. Yanagihara, K. Nishii, K. Inoue, N. Hirose, and T. Matsui, J. Vac. Sci. Technol. B **17**, 320 (1999).

[8] M. Tanabe, T. Matsuno, N. Kashiwagi, H. Sakai, K. Inoue, and A. Tamura, J. Vac. Sci. Technol. B **14**, 3248 (1996).

[9] J. B. Yoon, C. H. Han, E. Yoon, and C. K. Kim, Jpn. J. Appl. Phys., Part 1 **37**, 7081 (1998).

[10] G. H. Ryu, D. H. Kim, J. H. Lee, and K. S. Seo, IEEE Microwave Guid. Wave Lett. **10**, (2000).

[11] K. Y. Lim, D. J. Ripin, G. S. Petrich, L. A. Kolodziejski, E. P. Ippen, M. Mondol, and H. I. Smith, J. Vac. Sci. Technol. B **17**, 1171 (1999).

[12] H. Fujii, S. Kanemaru, T. Matsukawa, and J. Itoh, Appl. Phys. Lett. **75**, 3986 (1999).

[13] Y. K. Kwong, K. Lin, P. Hakonen, J. M. Parpia, and M. Isaacson, J. Vac. Sci. Technol. B **7**, 2020 (1989).

[14] H. G. Craighead, Science **290**, 1532 (2000).

[15] S. Y. Chou, P. R. Krauss, and P. J. Renstrom, Appl. Phys. Lett. **67**, 3114 (1995); Science **272**, 85 (1996).

[16] S. Y. Chou and P. R. Krauss, Microelectron. Eng. **35**, 237 (1997).

[17] H. Tan, L. Chen, M. Li, J. Wang, W. Wu and S. Y. Chou, The 44th International Conference on Electron, Ion and Photon Beam Technology and Nanofabrication, Palm Springs, CA, 30 May–2 June, 2000.